Three-flat test solutions based on simple mirror symmetry

Ulf Griesmann

In interferometric surface and wavefront metrology, three-flat tests are the archetypes of measurement procedures to separate errors in the interferometer reference wavefront from errors due to the test part surface, so-called absolute tests. What is believed to be a new class of solutions of the three-flat problem for circular flats is described in terms of functions that are symmetric or antisymmetric with respect to reflections at a single line passing through the center of the flat surfaces. The new solutions are simpler and easier to calculate than the known solutions based on twofold mirror symmetry or rotation symmetry. Strategies for effective azimuthal averaging and a method for determining the averaging error are also discussed.

OCIS codes: 120.3180, 120.3940, 220.4840.

1. Introduction

In interferometric metrology of precision surfaces and wavefronts, the system errors of the interferometer are often of the same magnitude as the form errors of the surface being measured. Procedures to separate the measurement errors of the interferometer from the form error of the surface under test, so-called absolute tests, are central to the testing of precision surfaces and wavefronts with interferometers. The archetype of an absolute test is the three-flat test, which is used to separate the flatness error of a nominally flat reference wavefront from the flatness error in the wavefront reflected by a test flat. Flat reference surfaces are used in many interferometers, and the test methods for flats are also applicable to spherical and some nonspherical surface and wavefront geometries. The following error separation method is also applicable outside interferometry whenever error separation for two-dimensional measurands is required.

In a Fizeau interferometer, a two-beam interferometer commonly used for form metrology of precision surfaces, reference surface S_R, and test surface S_T are arranged as shown in Fig. 1. The illumination system of the interferometer sends a collimated beam to a transmission flat with reference surface S_R, where a fraction of the beam is reflected. The transmitted fraction of the beam is partially reflected back by the test surface S_T. The reflected waves travel, coherently superimposed, to the detector where the surfaces are imaged, and the flatness error of the test wavefront relative to the reference wavefront is measured. In this paper, it is assumed that surfaces and wavefronts are described in part coordinates as indicated by the coordinate frames attached to the reference and test surfaces in Fig. 1. The combined wavefront $W(x, y)$, measured by the interferometer, is

$$W(x, y) = W_R(-x, y) + W_T(x, y), \tag{1}$$

where $W_R(x, y)$ stands for the wavefront reflected by the reference flat and $W_T(x, y)$ represents the wavefront reflected by the test surface. The negative sign for the x coordinate of the W_R term in Eq. (1) accounts for the rotation of the reference surface about the y axis by an angle π relative to the test surface. For the three-flat tests described here, it is also assumed that reference and test flats are circular with diameter d, and therefore $x^2 + y^2 \leq d^2/4$, with the origin of the coordinate system at the center of the flats.

With the Fizeau interferometer, flats can be compared in pairs, and the purpose of a flat test is a determination of the flatness error of each flat from pairwise comparisons of at least three flats. Three flats A, B, and C can be compared using the measurement sequence (BA, CA, CB) as shown in Fig. 2. In this paper, the convention is used that the first letter in a pair such as BA refers to the reference flat; the second letter refers to the test flat. The results of the three measurements, which have the same form as Eq. (1), are

U. Griesmann (ulf.griesmann@osa.org) is with the Manufacturing Engineering Laboratory, National Institute of Standards and Technology, 100 Bureau Drive, Gaithersburg, Maryland 20899-8223.

Received 17 January 2006; accepted 21 February 2006; posted 21 March 2006 (Doc. ID 67264).

0003-6935/06/235856-10$15.00/0

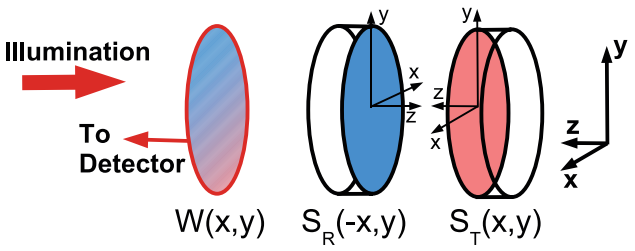

Fig. 1. (Color online) Reference surface S_R and test surface S_T in a Fizeau interferometer and coordinate system of the flat surfaces that are being compared. The coordinate system of the interferometer is indicated with bold arrows.

$$\begin{bmatrix} W_1(x,\,y) \\ W_2(x,\,y) \\ W_3(x,\,y) \end{bmatrix} = \begin{bmatrix} 1 & 0 & 1 & 0 \\ 1 & 0 & 0 & 1 \\ 0 & 1 & 0 & 1 \end{bmatrix} \begin{bmatrix} W_A(x,\,y) \\ W_B(x,\,y) \\ W_B(-x,\,y) \\ W_C(-x,\,y) \end{bmatrix}, \tag{2}$$

when written in matrix form (following Küchel[1]). In this equation, W_A, W_B, and W_C are the wavefronts reflected by the three flats, and W_1, W_2, and W_3 are the measurements of the relative wavefront errors.

Regardless of the order in which the flats are compared, at least one must serve as a reference and also as a test flat. In the example shown in Fig. 2, this is flat B, which leads to the well-known three-flat problem. Equation (2) can be solved only for the vertical line at $x = 0$ because, in the interferometer coordinate system, $W_B(x, y)$ and $W_B(-x, y)$ must be considered different variables and the coefficient matrix in Eq. (2) is rank deficient. It was proved many years ago that the three-flat problem cannot be solved by comparing more than three flats in the test.[2] A solution can only be found if at least one additional measurement is made.

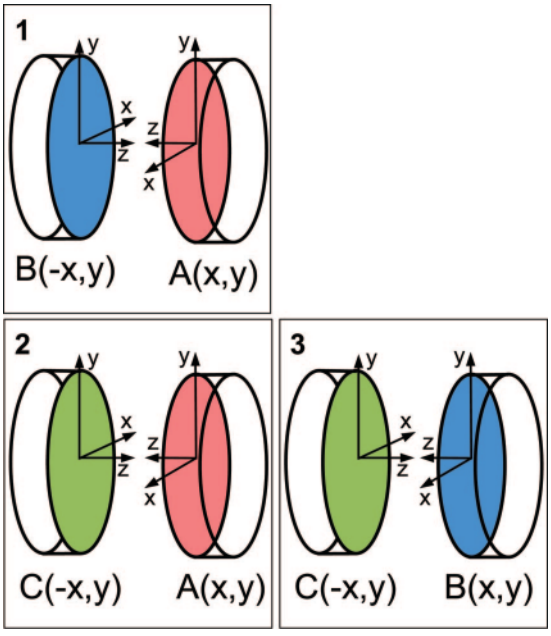

Fig. 2. (Color online) Measurement sequence (BA, CA, CB) for the comparison of three flats A, B, and C.

Over the past two decades, two important ideas have been developed that lead to approximate solutions for the three-flat problem. The first is the application of symmetries of the plane. The wavefronts in Eq. (2) can be split into parts W^I, which are invariant under a symmetry operation, and parts W^V, which change when the same symmetry operation is applied to them:

$$W(x,\,y) = W^I(x,\,y) + W^V(x,\,y). \tag{3}$$

When the symmetry operation is chosen such that $W^I(x, y) = W^I(-x, y)$ for all y, which means that the points $W(0, y)$ along the y axis do not change under the symmetry operation, the number of unknowns in Eq. (2) is reduced by one, and for the invariant component, Eq. (2) can be simplified to

$$\begin{bmatrix} W_1^I(x,\,y) \\ W_2^I(x,\,y) \\ W_3^I(x,\,y) \end{bmatrix} = \begin{bmatrix} 1 & 1 & 0 \\ 1 & 0 & 1 \\ 0 & 1 & 1 \end{bmatrix} \begin{bmatrix} W_A^I(x,\,y) \\ W_B^I(x,\,y) \\ W_C^I(x,\,y) \end{bmatrix}. \tag{4}$$

The inverse of the coefficient matrix in this equation exists and the invariant components of the three-flat wavefronts can be expressed in terms of the invariant components of the measurements:

$$\begin{bmatrix} W_A^I(x,\,y) \\ W_B^I(x,\,y) \\ W_C^I(x,\,y) \end{bmatrix} = \frac{1}{2} \begin{bmatrix} 1 & 1 & -1 \\ 1 & -1 & 1 \\ -1 & 1 & 1 \end{bmatrix} \begin{bmatrix} W_1^I(x,\,y) \\ W_2^I(x,\,y) \\ W_3^I(x,\,y) \end{bmatrix}. \tag{5}$$

In the Cartesian plane with Euclidian geometry, there are four kinds of symmetry: translations, reflections, rotations, and glide reflections, or glides. Glides combine a translation along a line with a reflection at the same line. For the circular flats discussed here, symmetries containing translations are not useful. Reflections and the subgroup of continuous rotations permit invariant functions $W^I(x, y)$, which satisfy the condition $W^I(x, y) = W^I(-x, y)$. These two symmetries can be used for solving the three-flat problem.

While symmetries make it possible to solve Eq. (2) for part of the wavefront flatness error, an additional concept must be introduced to find a solution for the part of the wavefront, which varies under symmetry operations. This is the concept of N-position averaging, summarized in Section 2, which was described by Evans and Kestner[3] and can be used to eliminate one of the unknown rotationally variant parts of the wavefronts and solve Eq. (2) for $W^V(x, y)$.

The use of mirror symmetry to solve the three-flat problem was originally suggested by Ai and Wyant,[4] who broke up wavefronts into symmetry components with respect to twofold mirror symmetry at the x and y axes. Later, Parks *et al.*[5] combined N-position averaging with twofold mirror symmetry to find solutions for the three-flat problem. Küchel[1] recently described a class of three-flat solutions in terms of

wavefront components, which are invariant and variant under continuous rotations.

In this paper, it is shown that a class of pixel-by-pixel solutions to the three-flat problem can be constructed in terms of functions that are symmetric and antisymmetric with respect to mirror operations at the y axis only. Solutions based on mirror symmetry at one line turn out to be the simplest solution of the three-flat problem and, in the analysis of measurement data, require minimal computational effort. A second orthogonal mirror line is not required. The only advantage of twofold mirror symmetry is that special measurement sequences with desirable statistical properties may be constructed.[1]

2. Azimuthal Average and *N*-Position Average

Before describing the solution of the three-flat problem, properties of the azimuthal average and its approximation through an N-position average are briefly reviewed because of the pivotal importance of these concepts in solving the three-flat problem. For a wavefront $W(r, \phi)$ in polar coordinates, defined on the interior of a circle with radius $d/2$, an operator $[\cdot]^R$ and a function $W^R(r)$ are defined:

$$W^R(r) \stackrel{\text{def}}{=} [W(r,\ \phi)]^R \stackrel{\text{def}}{=} \frac{1}{2\pi}\int_0^{2\pi} W(r,\ \phi)\mathrm{d}\phi. \quad (6)$$

The operator $[\cdot]^R$ is called the azimuthal averaging operator and $W^R(r)$ is the azimuthal average of $W(r, \phi)$. $W^R(r)$ does not depend on the azimuth angle ϕ; it is rotationally invariant. The azimuthal averaging operator, $[\cdot]^R$, is a projection operator because

$$[[W(r,\ \phi)]^R]^R = [W(r,\ \phi)]^R = W^R(r), \quad (7)$$

which follows directly from its definition in Eq. (6). The difference $\Omega(r, \phi) \stackrel{\text{def}}{=} W(r, \phi) - W^R(r)$ between the wavefront $W(r, \phi)$ and its azimuthal average $W^R(r)$ is the rotationally variant residuum of $W(r, \phi)$. Every wavefront $W(r, \phi)$ can be written as a sum of a rotationally invariant component and one that changes with rotation:

$$W(r,\ \phi) = W^R(r) + \Omega(r,\ \phi). \quad (8)$$

An important consequence of Eq. (7) is that the azimuthal average of the rotationally variant residuum vanishes identically:

$$[\Omega(r,\ \phi)]^R = \left[W(r,\ \phi) - W^R(r)\right]^R = W^R(r) - W^R(r) = 0. \quad (9)$$

When the azimuthal average of a sampled wavefront $W(r, \phi)$ is to be calculated with a computer, the integral in the definition of the azimuthal average Eq. (6) must be approximated by a sum. First, the integral in Eq. (6) can be written as the limit of a Riemann sum:

$$W^R(r) = \frac{1}{2\pi}\int_0^{2\pi} W(r,\ \phi)\mathrm{d}\phi = \lim_{N\to\infty}\left(\frac{1}{2\pi}\sum_{k=0}^{N-1} W(r,\ \phi_k)\Delta\phi_k\right). \quad (10)$$

When a constant angle increment $\Delta\phi = 2\pi/N$ is introduced, and the limit is approximated by a finite sum, the last equation becomes

$$W^R(r) \approx \frac{1}{N}\sum_{k=0}^{N-1} W(r,\ k\Delta\phi) \approx \frac{1}{N}\sum_{k=0}^{N-1} W(r,\ \phi - k\Delta\phi). \quad (11)$$

In the second line of Eq. (11), the constant function segments of the Riemann sum are replaced by the function segments $W(r, \phi)$ themselves. The approximation of the azimuthal average defined by Eq. (11) is called the N-position average of $W(r, \phi)$. It is calculated by rotating $W(r, \phi)$ N times by the angle $\Delta\phi = 2\pi/N$ and averaging the results. The N-position average is a periodic function in ϕ, with period $2\pi/N$. This is because in every angle interval $[2\pi k/N, 2\pi(k + 1)/N]$, $0 \le k \le N - 1$, the same segments of function $W(r, \phi)$ are averaged. For wavefronts sampled on a square grid, the angle increment $\Delta\phi$ must be chosen so that the increment at the edge of the image corresponds to twice the pixel spacing, which averages all the information contained in the sampled image. For a circular image with a radius of P pixels, $N \approx \pi P$ positions are needed. A circular image that just fills a detector array with 1000×1000 pixels requires 1570 rotations. Using a personal computer available in 2005, brute-force evaluation of Eq. (11) with so many rotations is unacceptably slow due to the large number of interpolations required for the image rotations. If N is not a prime number, one way of reducing the effort required to compute the N-position average is to factorize N into numbers that are not integer fractions of each other ($N = q_1 \cdot q_2 \cdot q_3, \ldots$), and to apply a sequence of N-position averages with $N = q_1, q_2, q_3, \ldots$ to the wavefront $W(x, y)$. The number of rotations required will generally be much smaller than N. For example, $N = 105$ can be factored into $3 \times 5 \times 7$. Equation (11) is applied first with $N = 7$ to $W(x, y)$ and then, in a second step, with $N = 5$ to the result of the first averaging procedure, and finally, in a third step, with $N = 3$ to the second intermediate result. After factorization, only 15 rotations of the function $W(x, y)$ need to be calculated instead of the 105 rotations required to calculate the 105-position average using Eq. (11) in one step, and, using a computer, it is easily confirmed that the results are practically identical. It is offered as conjecture that the result of this multistep N-position average is the same as applying Eq. (11) in one step. Another way of computing the N-position average is to transform $W(x, y)$ into polar coordinates, carry out the averaging in polar coordi-

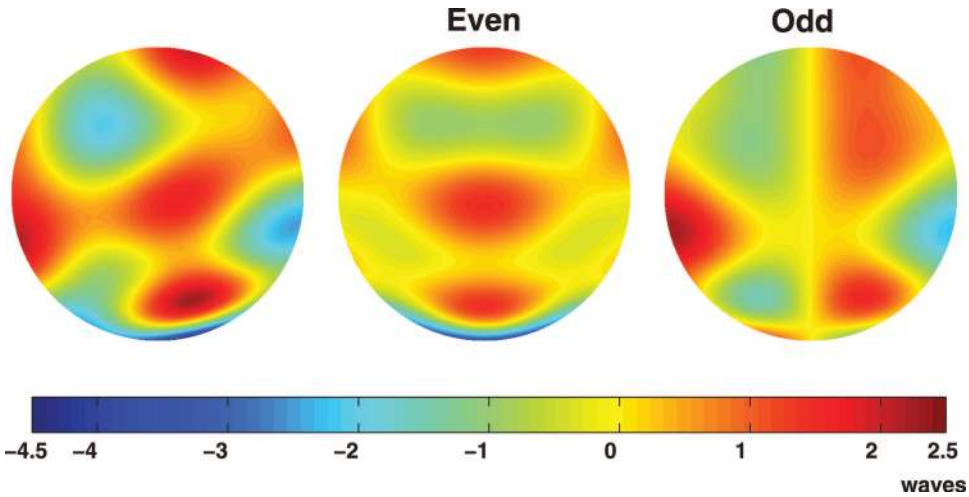

Fig. 3. (Color online) Function $W(x, y)$ and its decomposition into even (symmetric) and odd (antisymmetric) components. The coordinates are pixel numbers. The origin $(x, y) = (0, 0)$ is at the center of the images.

nates, and then transform the result back into the Cartesian coordinates of the original image. Since only two interpolation steps are required, and the averaging procedure in polar coordinates is a trivial operation, this is also much faster than calculating Eq. (11) in Cartesian coordinates. In practice, the implementation of the second approach may meet obstacles because image detectors sample on a square grid, and the software supplied with the interferometers usually does not provide for transformations of images into polar coordinates.

3. Mirror Symmetry

The simplest class of functions for which $W_B(-x, y) = W_B(x, y)$, with $-d/2 \le y \le d/2$, are functions that are invariant under reflection at the y axis. This suggests that wavefronts should be split into one part that is invariant under reflection at the y axis and another part that changes when it is mirrored. For a wavefront $W(x, y)$, an operator $[\cdot]^x$, and the mirrored function $W^x(x, y)$ are defined by

$$W^x(x, y) \stackrel{\text{def}}{=} [W(x, y)]^x \stackrel{\text{def}}{=} W(-x, y). \tag{12}$$

Two functions, $W^e(x, y)$ and $W^o(x, y)$,

$$W^e(x, y) \stackrel{\text{def}}{=} \frac{1}{2}\left[W(x, y) + W^x(x, y)\right],$$

$$W^o(x, y) \stackrel{\text{def}}{=} \frac{1}{2}\left[W(x, y) - W^x(x, y)\right], \tag{13}$$

are defined, which are, respectively, the even (symmetric) and odd (antisymmetric) components of $W(x, y)$ according to their behavior under reflections at the y axis:

$$\left[W^e\right]^x = W^e,$$

$$\left[W^o\right]^x = -W^o. \tag{14}$$

From here on, function arguments will be omitted when the meaning of an equation is clear without them. Obviously, every wavefront $W(x, y)$ can be written as a sum of a mirror-symmetric component and a nonsymmetric component:

$$W = W^e + W^o. \tag{15}$$

Figure 3 shows an example of a wavefront W and its decomposition into even and odd components. In solving the three-flat problem, the behavior of the even and odd symmetry components under azimuthal averages is of particular interest. When the functions in Eqs. (13) are split into components that are invariant and variant under rotation symmetry according to Eq. (8), the result is

$$W^e = \frac{1}{2}\left(W + W^x\right) = W^R + \frac{1}{2}\left(\Omega + \Omega^x\right),$$

$$W^o = \frac{1}{2}\left(W - W^x\right) = \frac{1}{2}\left(\Omega - \Omega^x\right). \tag{16}$$

Applying the azimuthal averaging operator, $[\cdot]^R$, to these equations, and using Eq. (9), results in

$$\left[W^e\right]^R = W^R,$$

$$\left[W^o\right]^R = 0. \tag{17}$$

The rotationally invariant part of the wavefront is entirely contained in the even wavefront component, and the azimuthal average of the odd wavefront component is zero.

4. Flat Tests

The three-flat problem is solved by adding one measurement to the sequence (BA, CA, CB) in which one

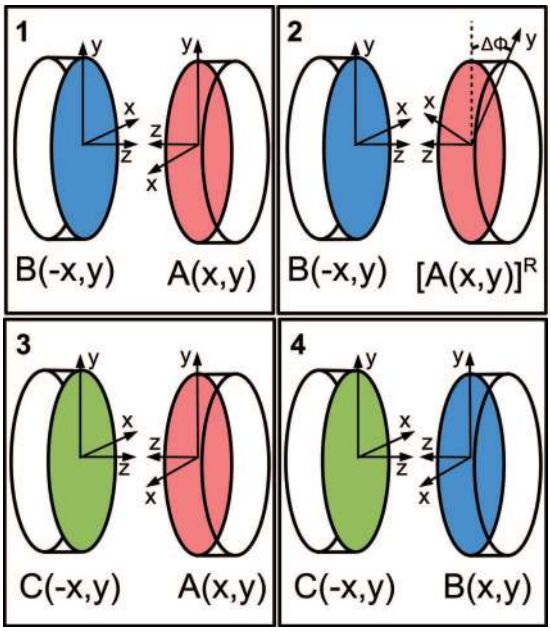

Fig. 4. (Color online) Measurement sequence comparing three flats, which can be solved for the flat surfaces.

of the flats is measured against the azimuthal average of the other flat. For example, in Fig. 4, which shows the modified measurement sequence (BA, BA^R, CA, CB), reference flat B is measured against the azimuthal average of test flat A. Recalling that the azimuthal average can be approximated by the N-position average [Eq. (11)], the measurement $W_2(x, y)$ in Fig. 4 can be realized by averaging N measurements of reference flat B against test flat A, in which A is rotated $N - 1$ times by $\Delta\phi = 2\pi/N$. It can easily be seen that this has the desired effect of measuring flat B against the azimuthal average of A, thus removing the rotationally variant component of flat A from $W_2(x, y)$ [see Eq. (9)]:

$$W_2(x, y) = \frac{1}{N}\sum_{k=0}^{N-1}\{W_B(-x, y) + [W_A(x, y)]^{k\Delta\phi}\} = W_B(-x, y) + \underbrace{\frac{1}{N}\sum_{k=0}^{N-1}[W_A(x, y)]^{k\Delta\phi}}_{\approx W_A^R(x, y)}. \quad (18)$$

The operator $[\cdot]^\Phi$ is used to indicate a rotation by an angle Φ.

The modified measurement sequence shown in Fig. 4 corresponds to the flat test equation

$$\begin{bmatrix} W_1(x, y) \\ W_2(x, y) \\ W_3(x, y) \\ W_4(x, y) \end{bmatrix} = \begin{bmatrix} 1 & 0 & 1 & 0 & 0 \\ 0 & 0 & 1 & 0 & 1 \\ 1 & 0 & 0 & 1 & 0 \\ 0 & 1 & 0 & 1 & 0 \end{bmatrix} \begin{bmatrix} W_A(x, y) \\ W_B(x, y) \\ W_B(-x, y) \\ W_C(-x, y) \\ [W_A(x, y)]^R \end{bmatrix}. \quad (19)$$

The vectors in this equation can be split into their even and odd components according to Eq. (15). For the right-hand side (rhs) vector of Eq. (19), the decomposition is

$$\begin{bmatrix} W_A(x, y) \\ W_B(x, y) \\ W_B(-x, y) \\ W_C(-x, y) \\ [W_A(x, y)]^R \end{bmatrix} = \begin{bmatrix} W_A^e(x, y) \\ W_B^e(x, y) \\ W_B^e(-x, y) \\ W_C^e(x, y) \\ W_A^R \end{bmatrix} + \begin{bmatrix} W_A^o(x, y) \\ W_B^o(x, y) \\ W_B^o(-x, y) \\ -W_C^o(x, y) \\ 0 \end{bmatrix}. \quad (20)$$

This leads to two equations, one for the even and one for the odd components of the wavefronts. The equation for the odd components is

$$\begin{bmatrix} W_1^o(x, y) \\ W_2^o(x, y) \\ W_3^o(x, y) \\ W_4^o(x, y) \end{bmatrix} = \begin{bmatrix} 1 & 0 & 1 & 0 \\ 0 & 0 & 1 & 0 \\ 1 & 0 & 0 & -1 \\ 0 & 1 & 0 & -1 \end{bmatrix} \begin{bmatrix} W_A^o(x, y) \\ W_B^o(x, y) \\ W_B^o(-x, y) \\ W_C^o(x, y) \end{bmatrix}. \quad (21)$$

Because the odd component of wavefront W_A is zero under azimuthal averaging [Eq. (17)], one of the variables in Eq. (19) is eliminated, and the matrix in Eq. (21) can be inverted. The solution for the odd wavefront components is

$$\begin{bmatrix} W_A^o(x, y) \\ W_B^o(x, y) \\ W_B^o(-x, y) \\ W_C^o(x, y) \end{bmatrix} = \begin{bmatrix} 1 & -1 & 0 & 0 \\ 1 & -1 & -1 & 1 \\ 0 & 1 & 0 & 0 \\ 1 & -1 & -1 & 0 \end{bmatrix} \begin{bmatrix} W_1^o(x, y) \\ W_2^o(x, y) \\ W_3^o(x, y) \\ W_4^o(x, y) \end{bmatrix}. \quad (22)$$

For the even components, one of the variables in Eq. (19) is eliminated because $W_B^e(-x, y) = W_B^e(x, y)$. The resulting equation for the even components is

$$\begin{bmatrix} W_1^e(x, y) \\ W_2^e(x, y) \\ W_3^e(x, y) \\ W_4^e(x, y) \end{bmatrix} = \begin{bmatrix} 1 & 1 & 0 & 0 \\ 0 & 1 & 0 & 1 \\ 1 & 0 & 1 & 0 \\ 0 & 1 & 1 & 0 \end{bmatrix} \begin{bmatrix} W_A^e(x, y) \\ W_B^e(x, y) \\ W_C^e(x, y) \\ W_A^R \end{bmatrix}, \quad (23)$$

which has the solution

$$\begin{bmatrix} W_A^e(x, y) \\ W_B^e(x, y) \\ W_C^e(x, y) \\ W_A^R \end{bmatrix} = \frac{1}{2}\begin{bmatrix} 1 & 0 & 1 & -1 \\ 1 & 0 & -1 & 1 \\ -1 & 0 & 1 & 1 \\ -1 & 2 & 1 & -1 \end{bmatrix} \begin{bmatrix} W_1^e(x, y) \\ W_2^e(x, y) \\ W_3^e(x, y) \\ W_4^e(x, y) \end{bmatrix}. \quad (24)$$

Using Eq. (15), even and odd components of the three wavefronts in Eqs. (22) and (24) can be added to get a single equation for three wavefront errors:

$$\begin{bmatrix} W_A \\ W_B \\ W_C \end{bmatrix} = \frac{1}{2}\begin{bmatrix} 1 & 1 & -1 & 2 & -2 & 0 & 0 \\ 1 & -1 & 1 & 2 & -2 & -2 & 2 \\ -1 & 1 & 1 & 2 & -2 & -2 & 0 \end{bmatrix}\begin{bmatrix} W_1^e \\ W_3^e \\ W_4^e \\ W_1^o \\ W_2^o \\ W_3^o \\ W_4^o \end{bmatrix}. \tag{25}$$

Equation (25) is the desired three-flat test solution that describes the wavefronts reflected by the three flats as linear combinations of the even (symmetric) and odd (antisymmetric) components of the measurements. Figure 5 is an illustration of this three-flat solution. The top row shows the simulated flatness errors of the three flats. For the purpose of illustrating the flat test, the wavefronts were generated by evaluating Zernike polynomials with 100 random coefficients, which are uniformly distributed in the interval [0, 1), even though in real flats the coefficients are not likely to be of similar magnitude. Off-center subapertures of the polynomials were then selected to generate wavefronts without the symmetry properties of the Zernike functions. Offsets and tilts are removed. A three-flat test was then simulated using the measurement sequence (BA, BA^R, CA, CB) as shown in Fig. 4; the azimuthal average was approximated with six-position averaging. The middle row of Fig. 5 shows the solution of the three-flat test using Eq. (25), and the difference between the true wavefronts and the flat test solutions is shown in the bottom row. The differences between the true wavefronts and the flat test solutions for all three flats are the same because only one flat, A, was rotated about the z axis in the test.

In practice, the measurement sequence (BA, BA^R, CA, CB) and its solution, Eq. (25), is useful when, for example, one of the flats is coated with a Clapham–Dew-type coating.[6] Such flats are used for testing flats with highly reflective coatings and can only serve as transmission flats. When the flatness errors of three nominally identical transmission flats are to be determined, it is preferable to use a variant of the test in which all flats undergo the same measurements and enter with the same statistical weight. An example of such a measurement sequence is (BA, BA^R, CB, CB^R, AC, AC^R). The equation describing this three-flat test is

$$\begin{bmatrix} W_1(x, y) \\ W_2(x, y) \\ W_3(x, y) \\ W_4(x, y) \\ W_5(x, y) \\ W_6(x, y) \end{bmatrix} = \begin{bmatrix} 1 & 0 & 0 & 0 & 1 & 0 & 0 & 0 & 0 \\ 0 & 0 & 0 & 0 & 1 & 0 & 1 & 0 & 0 \\ 0 & 1 & 0 & 0 & 0 & 1 & 0 & 0 & 0 \\ 0 & 0 & 0 & 0 & 0 & 1 & 0 & 1 & 0 \\ 0 & 0 & 1 & 1 & 0 & 0 & 0 & 0 & 0 \\ 0 & 0 & 0 & 1 & 0 & 0 & 0 & 0 & 1 \end{bmatrix} \times \begin{bmatrix} W_A(x, y) \\ W_B(x, y) \\ W_C(x, y) \\ W_A(-x, y) \\ W_B(-x, y) \\ W_C(-x, y) \\ [W_A(x, y)]^R \\ [W_B(x, y)]^R \\ [W_C(x, y)]^R \end{bmatrix}. \tag{26}$$

The solution proceeds along the lines laid out for Eq. (19). The vector of the wavefronts on the rhs of Eq. (26), written as sum of even and odd components, is

$$\begin{bmatrix} W_A(x, y) \\ W_B(x, y) \\ W_C(x, y) \\ W_A(-x, y) \\ W_B(-x, y) \\ W_C(-x, y) \\ [W_A(x, y)]^R \\ [W_B(x, y)]^R \\ [W_C(x, y)]^R \end{bmatrix} = \begin{bmatrix} W_A^e(x, y) \\ W_B^e(x, y) \\ W_C^e(x, y) \\ W_A^e(x, y) \\ W_B^e(x, y) \\ W_C^e(x, y) \\ W_A^R \\ W_B^R \\ W_C^R \end{bmatrix} + \begin{bmatrix} W_A^o(x, y) \\ W_B^o(x, y) \\ W_C^o(x, y) \\ W_A^o(-x, y) \\ W_B^o(-x, y) \\ W_C^o(-x, y) \\ 0 \\ 0 \\ 0 \end{bmatrix}. \tag{27}$$

The resulting equations for the even and odd components are solved in the same way as outlined in the solution for the measurement sequence (BA, BA^R, CA, CB). The solution for the even wavefront components is

$$\begin{bmatrix} W_A^e(x, y) \\ W_B^e(x, y) \\ W_C^e(x, y) \\ W_A^R \\ W_B^R \\ W_C^R \end{bmatrix} = \frac{1}{2}\begin{bmatrix} 1 & 0 & -1 & 0 & 1 & 0 \\ 1 & 0 & 1 & 0 & -1 & 0 \\ -1 & 0 & 1 & 0 & 1 & 0 \\ -1 & 2 & -1 & 0 & 1 & 0 \\ 1 & 0 & -1 & 2 & -1 & 0 \\ -1 & 0 & 1 & 0 & -1 & 2 \end{bmatrix} \times \begin{bmatrix} W_1^e(x, y) \\ W_2^e(x, y) \\ W_3^e(x, y) \\ W_4^e(x, y) \\ W_5^e(x, y) \\ W_6^e(x, y) \end{bmatrix}, \tag{28}$$

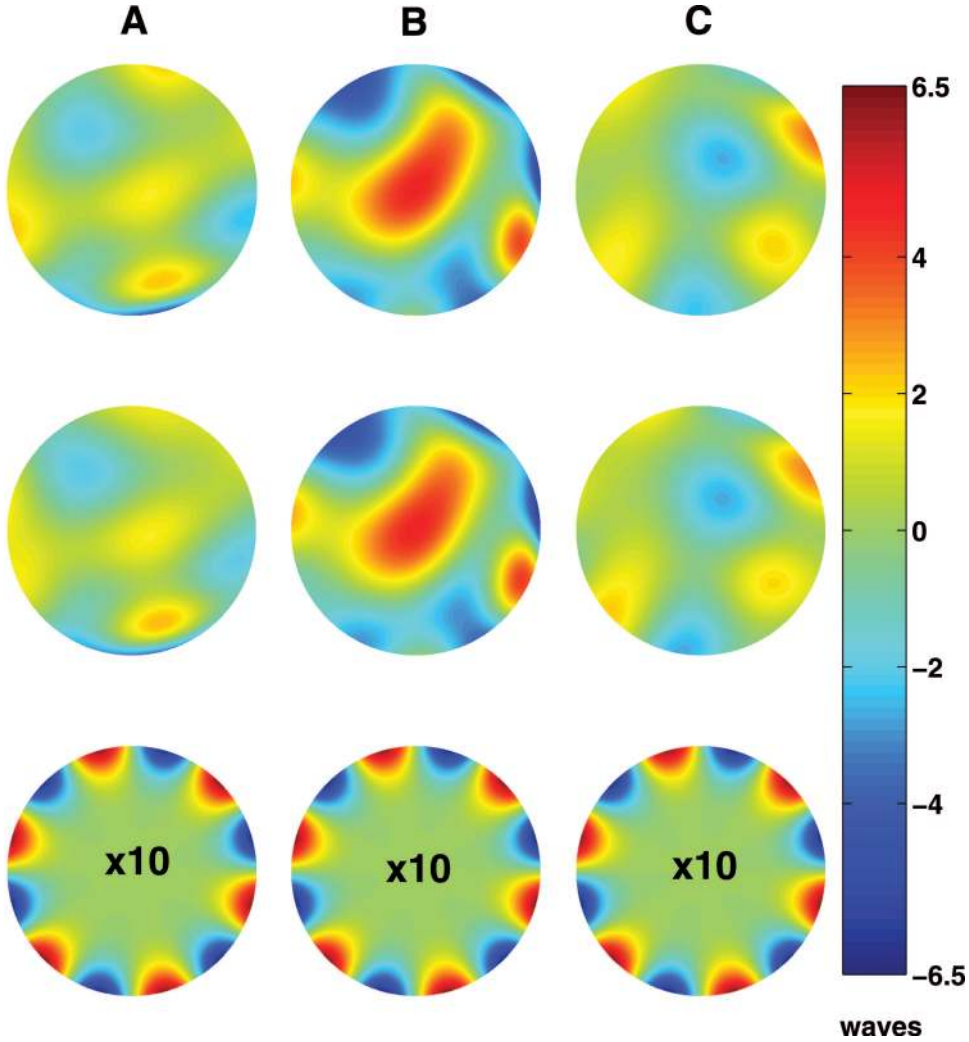

Fig. 5. (Color online) Simulation of a three-flat test based on simple mirror symmetry using Eq. (25) with six-position averaging. Top row, simulated flat wavefronts; middle row, flat solutions of the flat test; bottom row, difference between true wavefronts and the test solution. The coordinates are pixel numbers. The origin $(x, y) = (0, 0)$ is at the center of the images.

and the equation for the odd components has the solution

$$\begin{bmatrix} W_A^{\,o}(x, y) \\ W_B^{\,o}(x, y) \\ W_C^{\,o}(x, y) \\ W_A^{\,o}(-x, y) \\ W_B^{\,o}(-x, y) \\ W_C^{\,o}(-x, y) \end{bmatrix} = \begin{bmatrix} 1 & -1 & 0 & 0 & 0 & 0 \\ 0 & 0 & 1 & -1 & 0 & 0 \\ 0 & 0 & 0 & 0 & 1 & -1 \\ 0 & 0 & 0 & 0 & 0 & 1 \\ 0 & 1 & 0 & 0 & 0 & 0 \\ 0 & 0 & 0 & 1 & 0 & 0 \end{bmatrix} \begin{bmatrix} W_1^{\,o}(x, y) \\ W_2^{\,o}(x, y) \\ W_3^{\,o}(x, y) \\ W_4^{\,o}(x, y) \\ W_5^{\,o}(x, y) \\ W_6^{\,o}(x, y) \end{bmatrix}. \tag{29}$$

When the even and odd components of the solutions for W_A, W_B, and W_C are added, a single equation for the flatness errors of all three wavefront errors results:

$$\begin{bmatrix} W_A \\ W_B \\ W_C \end{bmatrix} = \frac{1}{2} \begin{bmatrix} 1 & -1 & 1 & 2 & -2 & 0 & 0 & 0 & 0 \\ 1 & 1 & -1 & 0 & 0 & 2 & -2 & 0 & 0 \\ -1 & 1 & 1 & 0 & 0 & 0 & 0 & 2 & -2 \end{bmatrix} \times \begin{bmatrix} W_1^{\,e} \\ W_3^{\,e} \\ W_5^{\,e} \\ W_1^{\,o} \\ W_2^{\,o} \\ W_3^{\,o} \\ W_4^{\,o} \\ W_5^{\,o} \\ W_6^{\,o} \end{bmatrix}. \tag{30}$$

The form of the coefficient matrix in Eq. (30) reflects

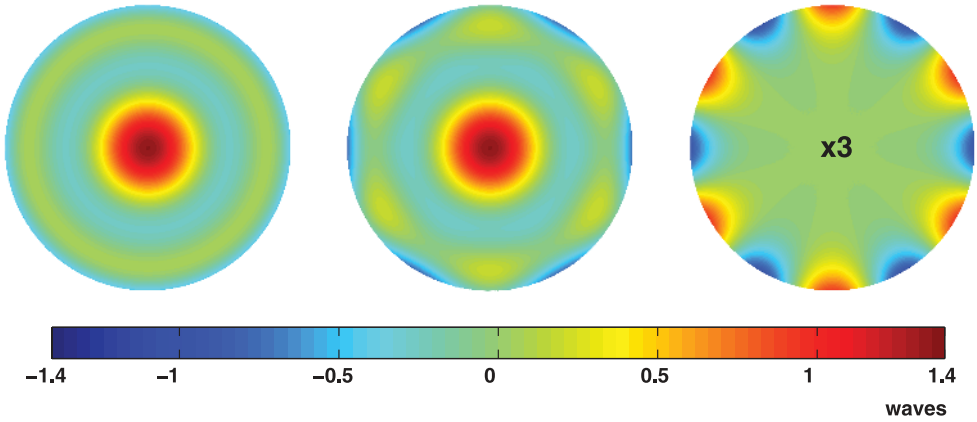

Fig. 6. (Color online) Rotationally invariant component of W_A, shown in the top left corner of Fig. 5, calculated with Eq. (35) (left) and with Eq. (33) (middle). The difference is shown on the right.

the nature of the measurement sequence in which all flats are treated identically. Equation (29) contains a second solution for the odd components of the wavefronts:

$$\begin{bmatrix} W_A^{\,o}(x,y) \\ W_B^{\,o}(x,y) \\ W_C^{\,o}(x,y) \end{bmatrix} = \begin{bmatrix} 0 & 0 & -1 \\ -1 & 0 & 0 \\ 0 & -1 & 0 \end{bmatrix} \begin{bmatrix} W_2^{\,o}(x,y) \\ W_4^{\,o}(x,y) \\ W_6^{\,o}(x,y) \end{bmatrix}. \quad (31)$$

When this solution for the odd components is added to the solution for the even components, an even simpler formula than Eq. (30) is found for the three-flat wavefronts:

$$\begin{bmatrix} W_A \\ W_B \\ W_C \end{bmatrix} = \frac{1}{2} \begin{bmatrix} 1 & -1 & 1 & 0 & 0 & -2 \\ 1 & 1 & -1 & -2 & 0 & 0 \\ -1 & 1 & 1 & 0 & -2 & 0 \end{bmatrix} \begin{bmatrix} W_1^{\,e} \\ W_3^{\,e} \\ W_5^{\,e} \\ W_2^{\,o} \\ W_4^{\,o} \\ W_6^{\,o} \end{bmatrix}. \quad (32)$$

Solutions for other measurement sequences, including ones with more than three flats, can be derived as needed using the mathematical recipe described in this section.

5. Efficient *N*-Position Averaging

In the simulation of the three-flat test shown in Section 4 (Fig. 5), the three-flat solutions differ from the true wavefronts because the six-position average is not a good approximation of the azimuthal average needed in the measurement W_2 of Eq. (19). In practical implementations of three-flat tests, true wavefronts are not known, but it is still possible to quantify the effectiveness of the approximation used for the azimuthal average. The solution for the even wavefront components, Eq. (24) in the previous section, also contains a solution for the rotationally invariant part of the wavefront of flat A, which was rotated in the measurement sequence (BA, BA^R, CA, CB):

$$W_A^{\,R} = W_2^{\,e} - \frac{1}{2}(W_1^{\,e} - W_3^{\,e} + W_4^{\,e}). \quad (33)$$

Similarly, in the case of the measurement sequence (BA, BA^R, CB, CB^R, AC, AC^R), the even solution, Eq. (28), also contains solutions for the rotationally invariant component of the three-flat wavefronts:

$$\begin{bmatrix} W_A^{\,R} \\ W_B^{\,R} \\ W_C^{\,R} \end{bmatrix} = \frac{1}{2} \begin{bmatrix} -1 & 2 & -1 & 0 & 1 & 0 \\ 1 & 0 & -1 & 2 & -1 & 0 \\ -1 & 0 & 1 & 0 & -1 & 2 \end{bmatrix} \begin{bmatrix} W_1^{\,e} \\ W_2^{\,e} \\ W_3^{\,e} \\ W_4^{\,e} \\ W_5^{\,e} \\ W_6^{\,e} \end{bmatrix}. \quad (34)$$

For the measurement sequence (BA, BA^R, CA, CB), an alternative way of calculating the rotationally invariant components of the wavefronts is to split the wavefronts into rotationally invariant and variant components and to solve Eq. (2) for the rotationally invariant components. In this case, a measurement against the azimuthal average of one of the flats is not needed. This leads to the following solution for the rotationally invariant wavefront components, as shown in the derivation of Eq. (5):

$$\begin{bmatrix} W_A^{\,R} \\ W_B^{\,R} \\ W_C^{\,R} \end{bmatrix} = \frac{1}{2} \begin{bmatrix} 1 & 1 & -1 \\ 1 & -1 & 1 \\ -1 & 1 & 1 \end{bmatrix} \begin{bmatrix} W_1^{\,R} \\ W_3^{\,R} \\ W_4^{\,R} \end{bmatrix}. \quad (35)$$

The rotationally invariant components of the measurements W_1, W_3, and W_4 on the rhs of Eq. (35) are calculated numerically from the measurement data using one of the methods discussed in Section 2. For these solutions, none of the flats need to be rotated.

The solution for the rotationally invariant component in Eq. (33) [and also in Eq. (34)], however, depends on a form of the N-position average, which involves actual rotations of a flat [see Eq. (18)]. The difference between the two solutions for the rotationally invariant wavefront component is a quantitative measure of the effectiveness of the N-position approximation that was performed in the measurements that lead to the solution in Eq. (33) [and Eq. (34)]. It can be used to determine the contribution of the approximation error to the uncertainty of the three-flat solution.

Clearly, a good approximation of the azimuthal average is essential for achieving a low uncertainty of the flat solutions. In the example of Fig. 5, the error in the approximation of the azimuthal average amounts to approximately 10% of the flatness errors in the flat wavefronts because relatively few rotation positions of flat A were used (see Fig. 6). Depending on the angular frequency content of the flatness errors, it may be necessary to average a large number of measurements to achieve a low uncertainty.

In this section, methods for the approximation of the azimuthal average are reviewed. As discussed in Section 3, Eq. (18), to average away the rotationally variant component of a wavefront from flat A, a series of measurements

$$\begin{aligned} W_\alpha &= W_B(-x,\, y) + W_A(x,\, y), \\ W_\beta &= W_B(-x,\, y) + [W_A(x,\, y)]^{\Delta\phi}, \\ &\vdots \end{aligned} \tag{36}$$

are made in which the test flat is repeatedly rotated by an angle of $\Delta\phi = 2\pi/N$. Greek letters are used as indices to avoid confusion with the measurement numbers introduced earlier in Eq. (2). When the differences between these measurements are considered,

$$W_\beta - W_\alpha = (W_A)^{\Delta\phi} - W_A, \tag{37}$$

it is found that the contribution of the stationary flat cancels out in all differences. From this, it follows, as Parks *et al.*[5] have shown, that the measurements $W_\gamma, \ldots, W_N$ in an N-position sequence can be calculated from the first two using the recursion relation

$$W_\kappa = W_{\kappa-1} + (W_\beta - W_\alpha)^{(\kappa-2)\Delta\phi}, \quad 3 \le \kappa \le N. \tag{38}$$

This recursion relation makes it possible to reduce the number of measurements needed to determine the N-position average Eq. (11) for as few as two measurements, independent of N, albeit at the cost of increased uncertainty. In practice, it will usually be desirable to make several measurements at several rotation positions to achieve a low measurement uncertainty for the difference $W_\beta - W_\alpha$, which is then used to calculate the remaining data sets using Eq. (38).

A different, but closely related, approach to removing the rotationally variant part from one of the wavefronts is found when the wavefronts in Eq. (37) are broken up into rotationally invariant and variant components using Eq. (8), which results in the equation

$$\Omega_A(r,\, \phi - \Delta\phi) - \Omega_A(r,\, \phi) = W_\beta - W_\alpha. \tag{39}$$

This equation is a difference equation for the rotationally variant part Ω_A of the flat that is rotated in the difference measurement, and it can be solved with standard methods. Once a solution for Ω_A has been found, the equation for W_2 in Eq. (18) can be rewritten as

$$W_2(x,\, y) = W_B(-x,\, y) + W_A(x,\, y) - \Omega_A(x,\, y) \tag{40}$$

because Ω_A is the wavefront component approximately removed by the N-position averaging. In a three-flat test, solving Eq. (39) is thus approximately equivalent to the application of N-position averaging [see Eq. (18)] to remove one of the odd wavefront components from Eq. (19).

The difference equation, Eq. (39), is solved by expressing Ω_A as a series and then solving the resulting algebraic equation for the coefficients of the series. Parks[7] and later Fritz[8] have described a method of solving Eq. (39) in which Ω_A is described by a (truncated) Zernike series. This method of solving Eq. (39) may be practical now because, with modern computers, it is possible to compute Zernike polynomials with large numbers of terms. An alternative, and equivalent, approach is to interpret the flat area as a set of concentric circles and find solutions on the circles using trigonometric polynomials. This solution for Eq. (39) was recently proposed by Freischlad.[9,10] A quantitative comparison of different three-flat test solution algorithms is currently under way in our laboratory.

I am indebted to my colleague Johannes Soons at the National Institute of Standards and Technology for many thought-provoking discussions and for shouldering most of the work on a MATLAB toolbox for the analysis of interferometry data, which was used for the simulation of three-flat tests and for the preparation of several figures.

References

1. M. F. Küchel, "A new approach to solve the three flat problem," Optik **112,** 381–391 (2001).
2. J. Schwider, "Ein Interferenzverfahren zur Absolutprüfung von Planflächennormalen II," Opt. Acta **14,** 389–400 (1967).
3. C. J. Evans and R. N. Kestner, "Test optics error removal," Appl. Opt. **35,** 1015–1021 (1996).
4. C. Ai and J. C. Wyant, "Absolute testing of flats by using even and odd functions," Appl. Opt. **32,** 4698–4705 (1993).

5. R. E. Parks, L. Shao, and C. J. Evans, "Pixel-based absolute topography test for three flats," Appl. Opt. **37,** 5951–5956 (1998).
6. P. Clapham and G. Dew, "Surface-coated reference flats for testing fully aluminized surfaces by means of a Fizeau interferometer," J. Sci. Instrum. **44,** 899–902 (1967).
7. R. E. Parks, "Removal of test optics errors," in *Advances in Optical Metrology I,* N. Balasubramanian and J. C. Wyant, eds., Proc. SPIE **153,** 56–63 (1978).
8. B. S. Fritz, "Absolute calibration of an optical flat," Opt. Eng. **23,** 379–383 (1984).
9. K. R. Freischlad, "Absolute interferometric testing based on reconstruction of rotational shear," Appl. Opt. **40,** 1637–1648 (2001).
10. R. P. Bourgeois, J. Magner, and H. P. Stahl, "Results of the calibration of interferometer transmission flats for the LIGO Pathfinder optics," in *Optical Manufacturing and Testing II,* H. P. Stahl, ed., Proc. SPIE **3134,** 86–94 (1997).